Study of the Inclusive Reaction $\gamma p \to \pi^- + (\text{Anything})$ with Polarized Photons at 2.8, 4.7, and 9.3 GeV*

K. C. Moffeit, J. Ballam, G. B. Chadwick, M. Della-Negra,† R. Gearhart, J. J. Murray, P. Seyboth,‡ C. K. Sinclair, I. O. Skillicorn, § H. Spitzer, ‖ and G. Wolf**
Stanford Linear Accelerator Center, Stanford University, Stanford, California 94305

and

H. H. Bingham, W. B. Fretter, W. J. Podolsky,** M. S. Rabin, A. H. Rosenfeld, R. Windmolders,†† and G. P. Yost
Department of Physics and Lawrence Berkeley Laboratory, University of California, Berkeley, California 94720

and

R. H. Milburn
Tufts University, Medford, Massachusetts 02155
(Received 10 December 1971)

We study the inclusive spectra of π^- mesons from the events obtained in three exposures of the SLAC 82-in. hydrogen bubble chamber to a nearly monochromatic polarized photon beam of mean energies 2.8, 4.7, and 9.3 GeV. The data are presented in terms of transverse momentum $p_\perp$ and three suggested choices for the other independent variable, i.e., the longitudinal momentum $p_\parallel$ in the laboratory system, the rapidity variable $y = \frac{1}{2}\ln[(E+p_\parallel)/(E-p_\parallel)]$, and the variable suggested by Feynman $x = p_\parallel^*/p_{\max}^*$ in the c.m. system. The 4π geometry of the bubble chamber allows us to cover the entire kinematically allowed range of these variables. We show that exact limiting fragmentation does not occur at our energies, but the data are compatible with an approach to a limiting distribution as $A + Bs^{-1/2}$. The qualitative features of the structure function $f(x, p_\perp^2)$ in terms of Feynman's x variable are similar at the three energies. Quantitatively, we find 5–10% differences between the 4.7- and 9.3-GeV data near $x=0$. We find $f(x, p_\perp^2)$ is not factorizable into independent functions of x and $p_\perp^2$. For our data the mean π^- multiplicity is described well by $\langle n^- \rangle = c^- \ln s + d^-$, where $c^- = 0.44 \pm 0.04$ and $d^- = 0.07 \pm 0.08$. Following the procedure suggested by Bali *et al.*, we calculate c^- from our experimentally observed 9.3-GeV structure function at $x=0$ and find $c^- = 0.44 \pm 0.02$ in agreement with the value obtained directly. We find a correlation between the azimuth of the π^- and the photon polarization plane only for $x > 0.3$ when elastic ρ^0 photoproduction is excluded. Lastly, we note that the distribution of π^- longitudinal momentum is not symmetric in the "quark frame" where $p_{\text{target}} = 1.5 p_{\text{beam}}$.

INTRODUCTION

We present a study of the inclusive reaction

$$\gamma p \to \pi^- + (\text{anything}) \tag{1}$$

at photon energies of 2.8, 4.7, and 9.3 GeV. Some data from a small exposure at 1.44 GeV are also given. The differential cross section for such a reaction can be written with the detected-particle phase space explicitly shown:

$$d^3\sigma = \frac{d^3p}{E} f_1(s, \vec{p}), \tag{2}$$

where $\vec{p}$ and E are the momentum and energy of the pion and s is the center-of-mass energy squared. It has been suggested[1-4] that the structure function, $f_1(s, \vec{p})$, when expressed in terms of an appropriate set of variables should have a simple form at large s. Three sets of variables have been proposed:

i. Longitudinal momentum. Benecke *et al.*[1] have proposed the use of $p_\parallel$, the longitudinal momentum of the produced pion in the laboratory frame. At large s they suggest that $f_1(s, \vec{p})$ of Eq. (2) should be independent of s for small $p_\parallel$.

ii. The rapidity variable. Feynman[2] has proposed the use of the variables $p_\perp$ and y, where $p_\perp$ is the transverse momentum of the pion and

$$y = \tfrac{1}{2}\ln\left(\frac{E+p_\parallel}{E-p_\parallel}\right) \tag{3}$$

is the "rapidity." Here, the energy E and $p_\parallel$ are evaluated in the laboratory frame. After an integration over the azimuthal distribution of the π^-, Eq. (2) becomes simply

$$d^2\sigma = dy\, dp_\perp^2 \pi f_2(s, y, p_\perp^2), \tag{4}$$

i.e., the denominator E is incorporated into dy. The multiperipheral model predicts that in this set of variables, the structure function should

have a simple form at large s; namely, that it becomes independent of s for y near its minimum and maximum values and that for central y values $f_2(s, y, p_\perp^2)$ is a function of $p_\perp^2$ only.[3,4]

iii. Feynman x variable. Feynman has suggested that the structure function of Eq. (2) "scales" at high energy. That is, as $s \to \infty$, it becomes a function only of $p_\perp^2$ and the ratio $x = p_\parallel^*/p_{\max}^*$, where $p_\parallel^*$ is the c.m. longitudinal pion momentum and $p_{\max}^*$ is the maximum c.m. pion momentum.[5] The differential cross section, Eq. (2), in terms of these variables, becomes

$$d^2\sigma = \pi \frac{p_{\max}^*}{E^*} dx dp_\perp^2 f_3(x, p_\perp^2, s), \tag{5}$$

where E^* is the c.m. energy of the pion.

To illustrate the connection between the variables we give in Fig. 1 the relation between $p_\parallel$ in the laboratory and the variables x [Fig. 1(a)] and y [Fig. 1(b)] for our 9.3-GeV data. The upper boundary for $p_\parallel > 0$ in both cases corresponds to $p_\perp = 0$; points above the kinematic boundary in Fig. 1(a) are due to the finite width of the photon energy spectrum. The scatter plot of x and y shown in Fig. 1(c) displays how the region near $x = 0$ is expanded when expressed in terms of y. The 4π geometry of the bubble chamber allows us to cover the entire kinematically allowed range of these variables.

At high energies Vander Velde[6] has shown that an energy-independent distribution in $f_1(p_\parallel, p_\perp^2)$ for target-fragmented pions results in a structure function $f_3(x, p_\perp^2)$ which is independent of s for the corresponding x region. However, this equivalence is not valid for the photon energies used here.

In this paper we present our data in terms of the three sets of variables discussed above. We study the characteristics of the structure function in order to: (a) determine if any of these sets of variables give a simple description, like that expected in the high-energy region, at our moderate photon energies; (b) determine the dependence of the structure function on these variables; (c) investigate the dependence of the average pion multiplicity on s; and (d) compare inclusive pion photoproduction with that from hadronic reactions.

EXPERIMENTAL PROCEDURES

We have studied photoproduction of hadrons using a nearly monochromatic polarized photon beam at 2.8, 4.7, and 9.3 GeV in the 82-in. LBL-SLAC hydrogen bubble chamber. We have obtained 92, 150, and 138 events/μb at the three energies, respectively. Figure 2 shows the photon energy spectra at the three energies; the energy resolution is ±(3–4)%. The low-energy tail of the spectrum gives <2.5% of the π^- mesons produced. Furthermore, in the case of 3-constraint events (no outgoing neutrals), we fitted for E_γ and rejected low-energy events.

We used all well-measured 3-, 5-, 7-, and 9-

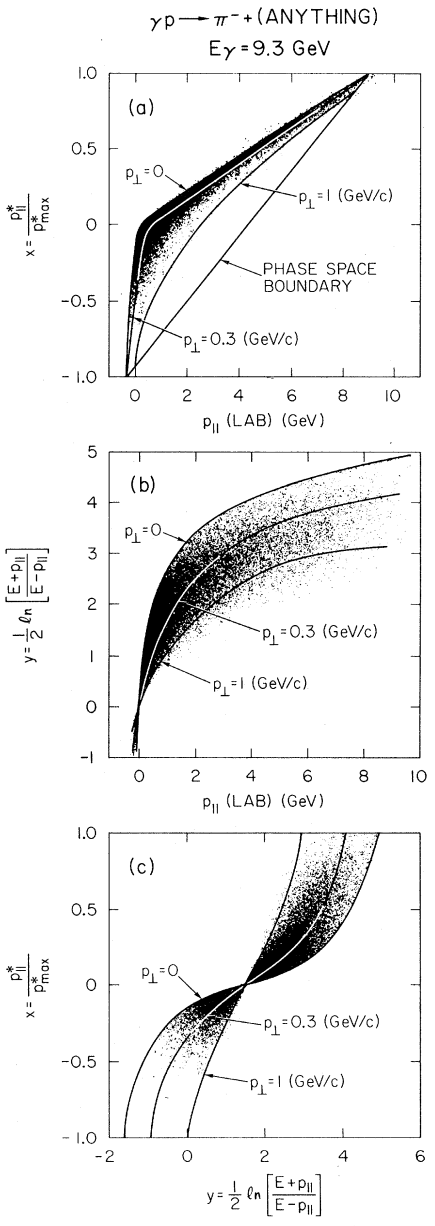

FIG. 1. (a) Scatter plot of π^- longitudinal momentum $p_\parallel$ in the laboratory frame and $x = p_\parallel^*/p_{\max}^*$ in the c.m. system for the 9.3-GeV data. (b) Scatter plot of π^- longitudinal momentum $p_\parallel$ and the rapidity $y = \frac{1}{2}\ln[(E + p_\parallel)/(E - p_\parallel)]$ in the laboratory frame. (c) Scatter plot of $y = \frac{1}{2}\ln[(E + p_\parallel)/(E - p_\parallel)]$ and $x = p_\parallel^*/p_{\max}^*$. The curves in each case show contours of constant transverse momentum calculated for $E_\gamma = 9.3$ GeV.

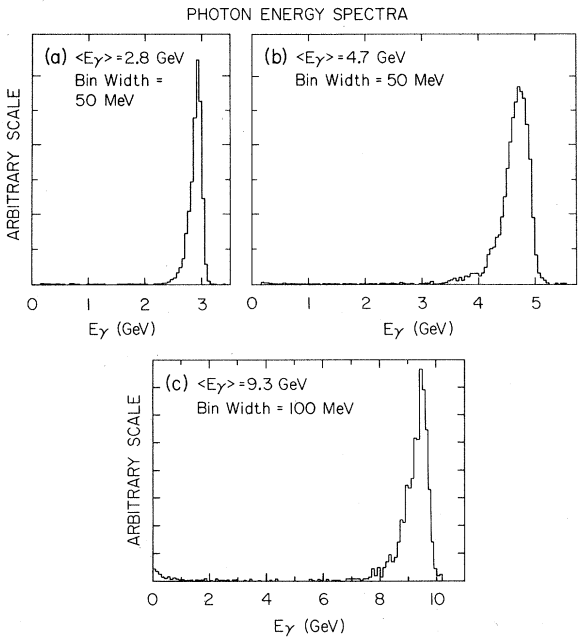

FIG. 2. Photon energy spectra for the exposures at (a) 2.8, (b) 4.7, and (c) 9.3 GeV.

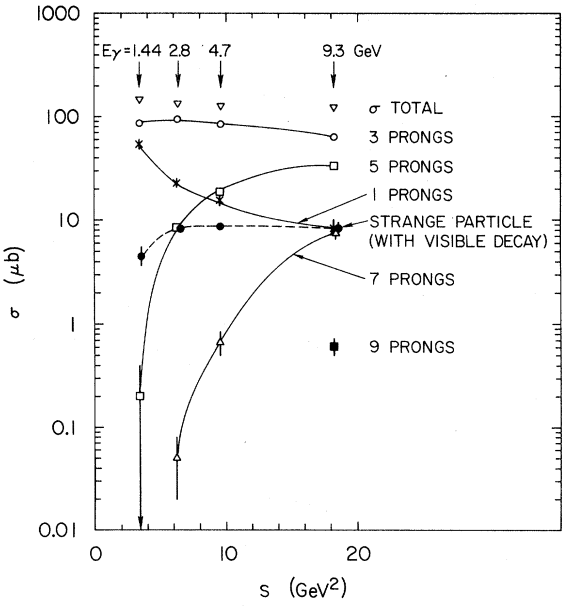

FIG. 3. Total and topological photoproduction cross sections versus the center-of-mass energy squared s. The lines are provided only to help distinguish between topologies.

prong events; 1-prong events do not have a negative track. Each topology was weighted separately for its fraction of unmeasurable events. There is a small contamination from unidentified K^- mesons which we estimate to be $(0.5 \pm 0.5)\%$, $(2 \pm 2)\%$, and $(3 \pm 3)\%$ at 2.8, 4.7, and 9.3 GeV, respectively. Events having an identified strange particle were not included in this study.[7] The fractions of π^- mesons from these events are estimated to be $(1.3 \pm 0.2)\%$, $(2.9 \pm 0.2)\%$, and $(4.3 \pm 0.2)\%$ at 2.8, 4.7, and 9.3 GeV. We have not applied these two roughly compensating (in numbers) types of corrections to the distributions given in this paper unless otherwise stated.

All photographs were scanned at least twice, giving over-all scanning losses of $\lesssim 1\%$. However, we found greater losses in the reaction $\gamma p \to \pi^+\pi^- p$ at small momentum transfers; in addition this reaction has some contamination from wide-angle e^+e^- pairs. All events giving an accepted fit to $\gamma p \to \pi^+\pi^- p$ were used in this study and a total correction to the channel $\gamma p \to \pi^+\pi^- p$ of $(-1 \pm 1)\%$, $(+5 \pm 1)\%$, $(+2 \pm 1)\%$ at 2.8, 4.7, and 9.3 GeV is included in the results reported here. We estimate systematic uncertainties in the cross sections to be less than 3%.

CROSS SECTIONS

We show in Fig. 3 the total photoproduction cross section[8] versus the center-of-mass energy squared at our three energies; also shown are the results of a small exposure made at 1.44 GeV. Although the total cross section is approximately constant in this energy region, the topological cross sections as seen from Fig. 3 vary rapidly with energy. The cross sections for larger multiplicities increase with energy. A similar behavior is found in πp, Kp, and pp interactions.[9]

LONGITUDINAL-MOMENTUM DISTRIBUTION IN THE LABORATORY

The hypothesis of limiting fragmentation put forward by Benecke *et al.*[1] suggests that the spectra of low-momentum particles become independent of the beam energy as the beam energy becomes large. To test if this hypothesis holds at our energies we give in Fig. 4

$$\mathcal{F}(p_\parallel) = \int_0^\infty \left(E \frac{d^2\sigma}{dp_\perp^2 dp_\parallel}\right) dp_\perp^2$$

in the laboratory frame for inclusive π^- production. The structure function rises rapidly from $p_\parallel < 0$ (backward production) to $p_\parallel \sim 500$ MeV/c followed by a more gradual falloff at high pion momenta. For small $p_\parallel$ (target fragmentation region) the curves are qualitatively the same; however, as seen in the insert of Fig. 4, the structure function at 9.3 GeV for $p_\parallel < 300$ MeV/c is lower by 10–30% (2–5 standard deviations at every point) than at 4.7 GeV. This means that in the laboratory system we do not observe exact limiting fragmentation in $\mathcal{F}(p_\parallel)$ at our energies.[10]

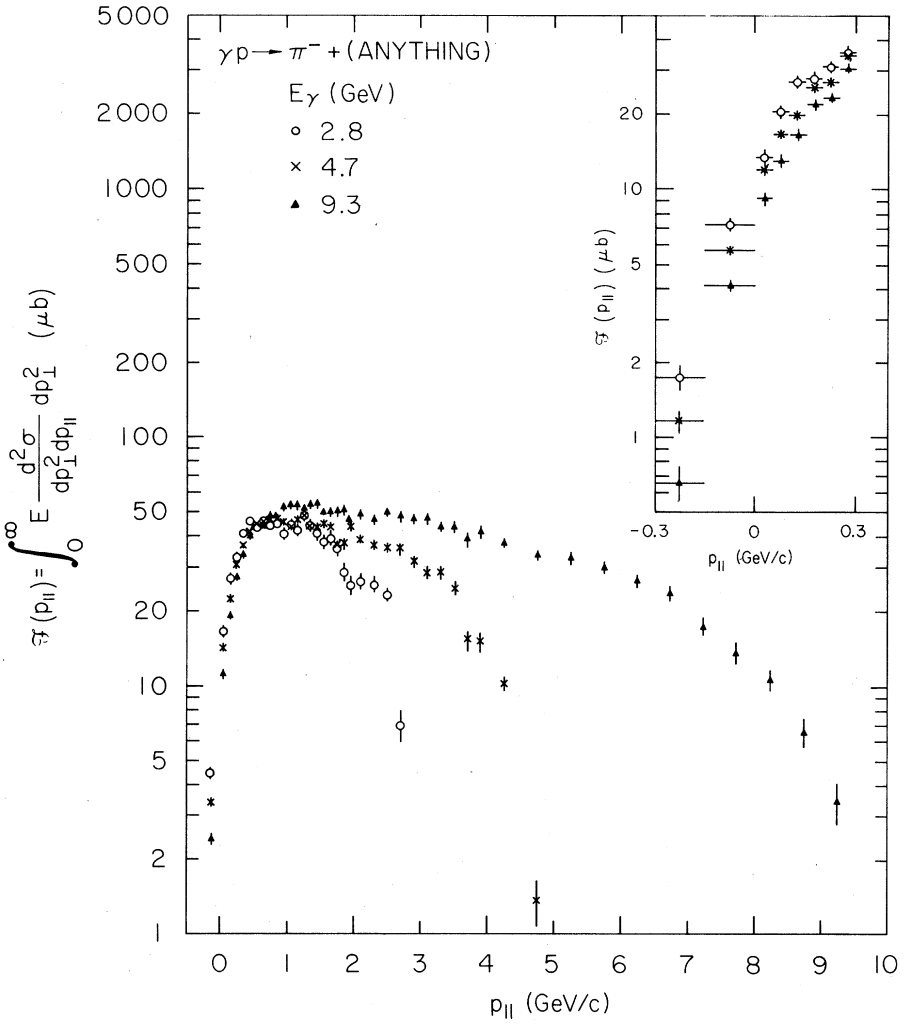

FIG. 4. Structure function $\mathcal{F}(p_{\parallel})$ in the laboratory frame at 2.8, 4.7, and 9.3 GeV for $\gamma p \to \pi^- + (\text{anything})$. The insert shows the region $p_{\parallel} < 300$ MeV/c on an expanded scale.

To demonstrate further the energy dependence we show in Fig. 5 the dependence of the structure function on the square of the transverse momentum, $p_\perp{}^2$, in the region near $p_{\parallel}(\text{lab}) = 0$. Again, we find the 9.3-GeV data systematically lower than the 4.7-GeV results.

Mueller[11] has suggested that the single-particle distributions in the inclusive reaction $a+b \to c+(\text{anything})$ can be related to the forward elastic three-body amplitude $a+b+\bar{c} \to a+b+\bar{c}$. Assuming that this amplitude is dominated by the usual Regge singularities, (i) the Pomeranchuk trajectory with $\alpha_P(0)=1$ and (ii) the approximately exchange-degenerate meson trajectories ($\rho, P'=f, \omega, A_2$) with $\alpha_M(0) \simeq 0.5$, Chan *et al.*[12] predict that the invariant cross section should reach a limiting distribution as $A+Bs^{-1/2}$, where A and B are independent of s. In order to test this prediction we give in Fig. 6 $\mathcal{F}(p_{\parallel}, s)$ for various intervals in $p_{\parallel}$ versus $s^{-1/2}$. Our data are consistent with the predicted $s^{-1/2}$ dependence.

Using the duality hypothesis, Chan *et al.*[12] also suggest that when the quantum numbers of the three-body system $a+b+\bar{c}$ are exotic a limiting distribution will be obtained at lower energies than if $a+b+\bar{c}$ were nonexotic. This means that reactions such as

$$p+p \to \pi^- + (\text{anything}),$$

$$K^+ + p \to \pi^- + (\text{anything}),$$

$$\pi^+ + p \to \pi^- + (\text{anything})$$

which have exotic quantum numbers in $ab\bar{c}$ (i.e., $pp\pi^+$, $K^+p\pi^+$, $\pi^+p\pi^+$) will approach limiting behavior more rapidly than

$$\pi^- + p \to \pi^- + (\text{anything}),$$

$$\gamma + p \to \pi^- + (\text{anything})$$

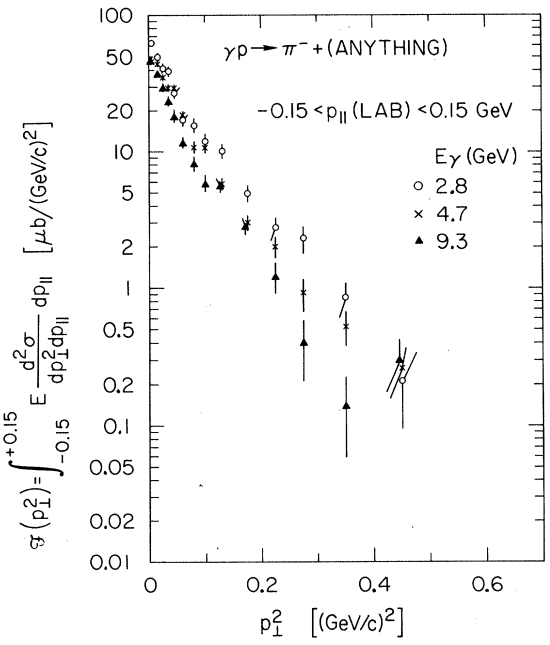

FIG. 5. Structure function $\mathcal{F}(p_\perp^2)$ for $-0.15 < p_\parallel(\text{lab}) < 0.15$ GeV/c at 2.8, 4.7, and 9.3 GeV.

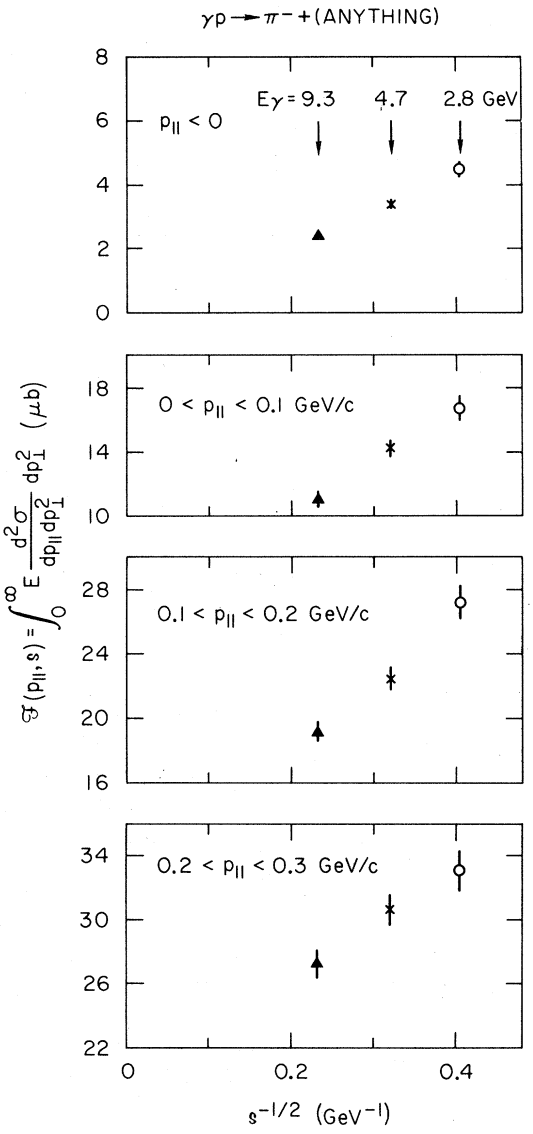

FIG. 6. Structure function $\mathcal{F}(p_\parallel, s)$ in the laboratory for labeled intervals in $p_\parallel$ versus $s^{-1/2}$.

which are nonexotic (i.e., $\pi^- p\pi^+$ and $\gamma p\pi^+$).

To compare the pion spectra from photoproduction with those from hadron-induced reactions we normalize the distributions by dividing by the asymptotic total cross section of each reaction, as suggested by Chan *et al.*[12] Figure 7 shows

$$\frac{1}{\sigma_{\text{tot}}(\infty)}\frac{d\sigma}{dp_\parallel}$$

in the laboratory frame for our 9.3-GeV photoproduction data together with the results of Chen *et al.*[13,14] The normalized π^- cross sections from the "exotic" pp, K^+p, and π^+p reactions agree but are a factor 2 smaller than the π^- cross sections from the "nonexotic" $\pi^- p$ and γp reactions. We note that the π^- cross sections from photoproduction and the $\pi^- p$ reaction are remarkably similar.

THE RAPIDITY VARIABLE

The introduction of the rapidity variable, y, results in the following simplifications for the structure function $f_2(s, y, p_\perp^2)$:

(a) The differential cross section is simply related to the structure function without a phase-space factor,

$$d^2\sigma = dy\,dp_\perp^2 \pi f_2(s, y, p_\perp^2).$$

(b) Under a Lorentz boost along the beam axis, y transforms into $y + \ln\gamma(1+\beta)$, where γ and β define the boost. Therefore, the form of the structure function is invariant under boost; it is only translated in y.

Arguing from two fundamental multiperipheral concepts, (a) that transverse momenta are limited and (b) that distant particles on the multiperipheral chain are uncorrelated, Wilson[3] and DeTar[4] predict that at sufficiently high incident energies, the function $f_2(y, p_\perp^2, s)$ has three characteristic features:

(i) An energy-independent limiting behavior of

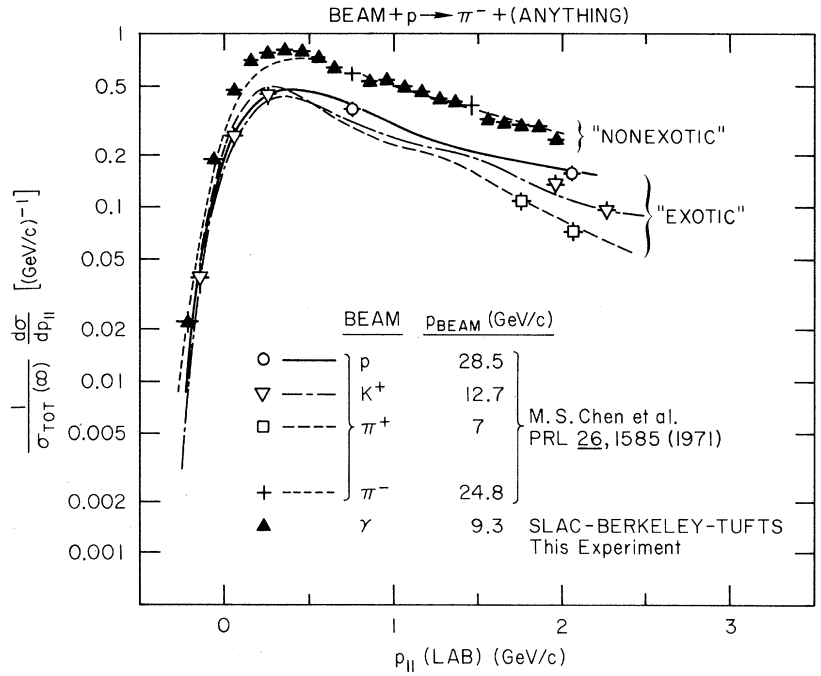

FIG. 7. Longitudinal-momentum distributions $d\sigma/dp_{\parallel}$ in the laboratory system normalized to the total cross sections at $s=\infty$ for hadron-induced reactions compared with our photoproduction results at 9.3 GeV. Curves are polynomial fits to the hadron-induced data with representative data points shown (as provided by the authors quoted).

$f_2(y,p_\perp^2)$ is expected as the total energy is increased, for $(y-y_{\min})$ or $(y_{\max}-y)$ sufficiently small. This corresponds to limiting fragmentation of the target (region I of Fig. 8) and the beam particle (region III of Fig. 8), respectively.

(ii) Fragmentation of the target is independent of the beam particle and *vice versa*.

(iii) The central region (labeled II in Fig. 8) of the spectrum is independent of both beam and target particles; it is independent of y and its width increases logarithmically with increasing energy.

At sufficiently high energy the above features also follow from Feynman's parton model.[2]

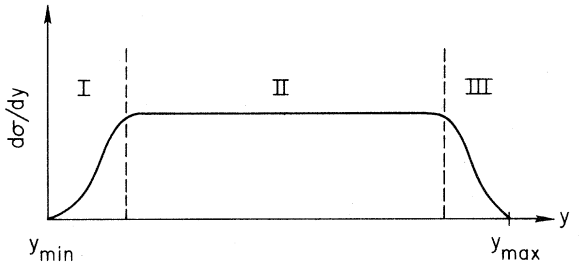

FIG. 8. Sketch of the general features of the "rapidity" variable distribution $d\sigma/dy$ for secondary particles as predicted by the multiperipheral model. The labels I, II, and III correspond to the target, central, and beam regions, respectively, discussed in the text.

In Fig. 9 we show the scatter plot in y and $p_\perp^2$ at 9.3 GeV for the π^- of reaction (1). The boundaries imposed by the kinematical constraints at small and large y values are clearly visible. The points concentrate at small $p_\perp^2$ and at y near its central

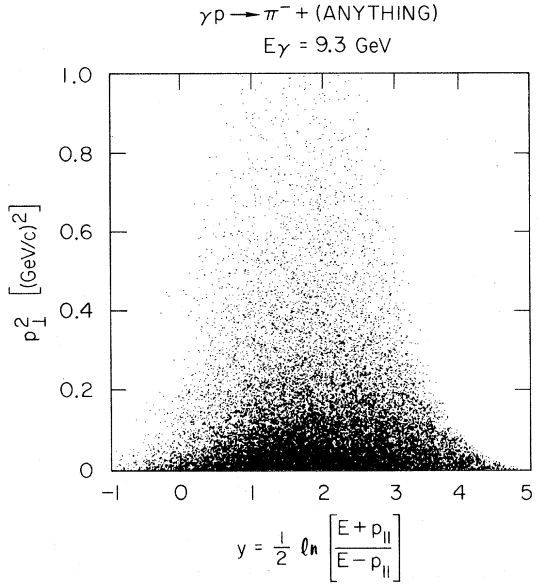

FIG. 9. $\gamma p \to \pi^- +$ (anything) at 9.3 GeV: Scatter plot of the rapidity variable y in the laboratory frame versus transverse momentum squared $p_\perp^2$.

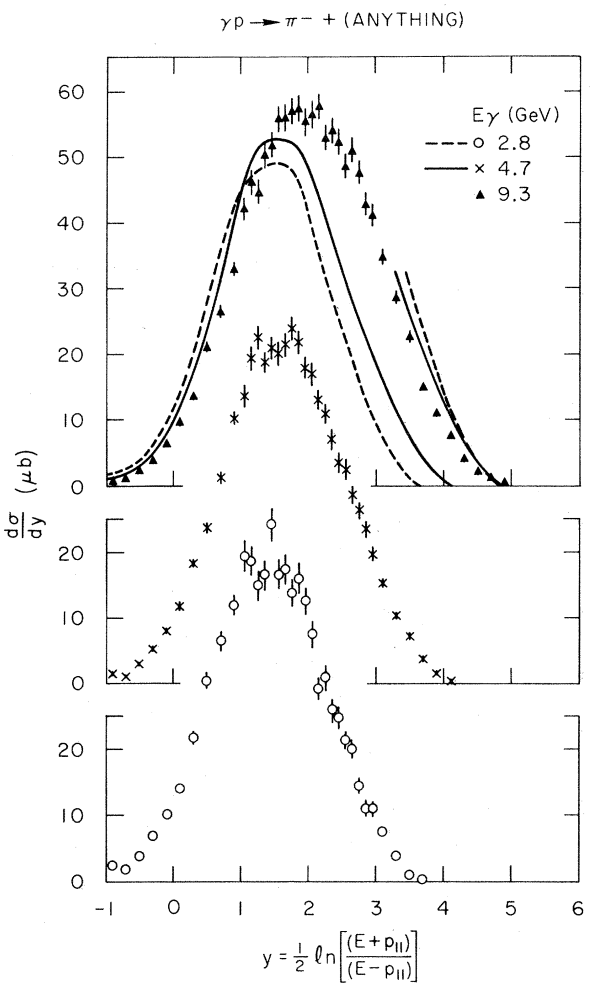

FIG. 10. Reaction $\gamma p \to \pi^- + (\text{anything})$: Differential π^- cross section $d\sigma/dy$. The solid and broken bell-shaped curves superimposed on the 9.3-GeV data represent the 2.8- and 4.7-GeV data beneath, having the same $y_{\min}$ while the partial curves are the lower-energy data transposed to have the same $y_{\max}$.

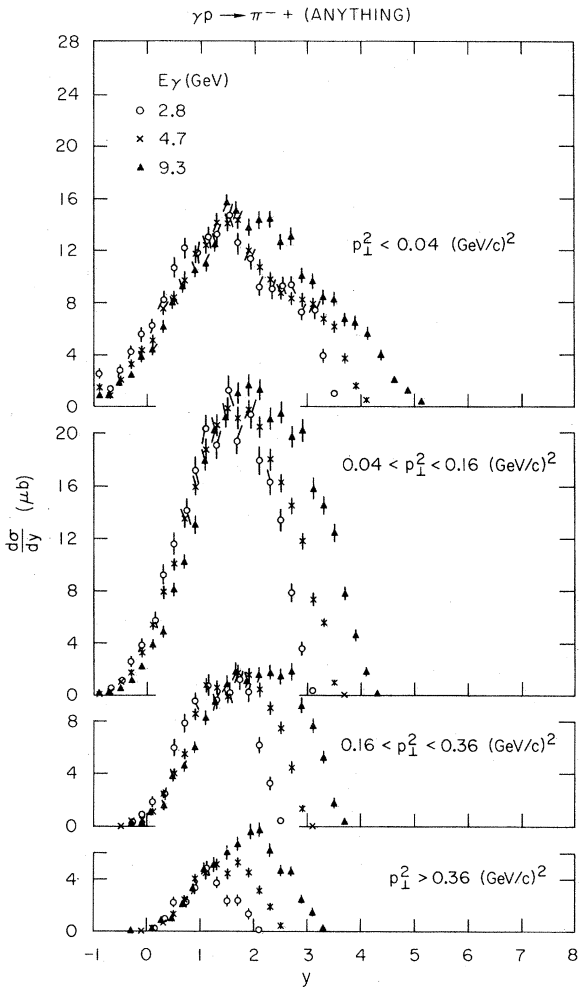

FIG. 11. Reaction $\gamma p \to \pi^- + (\text{anything})$: Differential π^- cross section $d\sigma/dy$ for various intervals in the transverse momentum at 2.8, 4.7, and 9.3 GeV.

value. In Fig. 10 we show $d\sigma/dy$; in particular, no extended flat region is observed (region II of Fig. 8).[16] For the three energies we find roughly Gaussian distributions in $d\sigma/dy$ whose width increases with increasing energy. Furthermore, we find in the target region (small y) a significant decrease in $d\sigma/dy$ with increasing photon energy (e.g., from Fig. 10 at $y = 0.5$ the 9.3-GeV value is ~20% lower than the 4.7-GeV result). We conclude that we do not have exact limiting target fragmentation at our energies. To test limiting fragmentation of the beam region we compare $d\sigma/dy$ at an equal distance from $y_{\max}$. Figure 10 shows that $d\sigma/dy$ at $(y - y_{\max})$ also decreases with increasing photon energy.

In Fig. 9 we saw clearly how the kinematic boundary narrows the range in y as transverse momentum increases. Thus, a flat distribution in

$$\frac{d^2\sigma}{dy\,dp_\perp{}^2}$$

will not result in a flat $d\sigma/dy$ when integrated over all transverse momenta. In Fig. 11 we give $d\sigma/dy$ for various intervals of transverse momenta. At 2.8 and 4.7 GeV no extended flat region is observed even when $p_\perp{}^2$ is restricted to a narrow interval; at 9.3 GeV the data are inconclusive.

The absence of a flat region in $d\sigma/dy$ would not be surprising at our energies in view of the following argument. We assume that the influence of the target fragmentation π^- is given by the kinematic region in which significant production of nucleon resonances at the nucleon vertex occurs. Nucleon resonance production occurs for masses

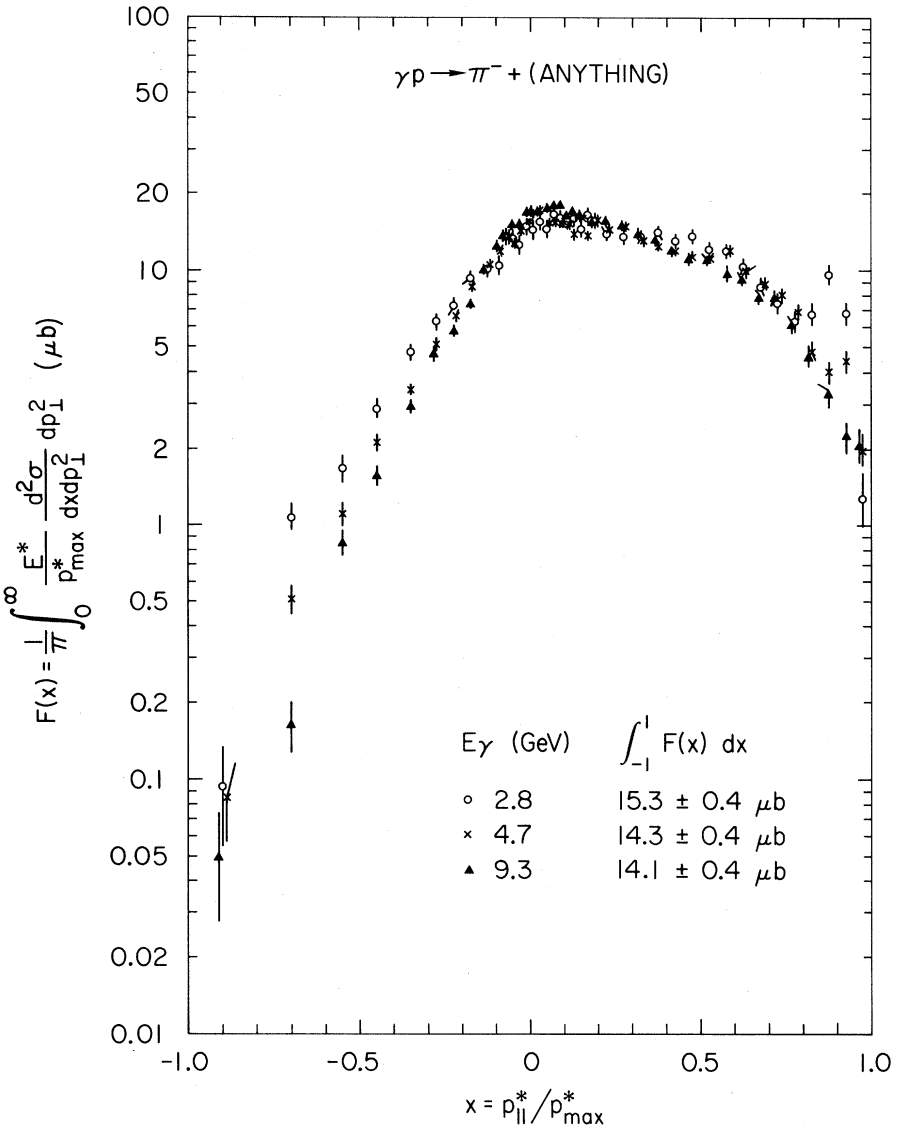

FIG. 12. Reaction $\gamma p \to \pi^-$ + (anything): Structure function $F(x)$ for $E_\gamma = 2.8$, 4.7, and 9.3 GeV.

up to 2 GeV corresponding to π^- laboratory momenta from the resonance decay up to ~1 GeV and hence to values of y up to 2.7. Therefore, the target fragmentation region can be expected to extend up to values of $y = 2$ to 3. On the other hand we observe that the ρ^0's which are elastically produced by fragmentation of the beam photons influence the y distribution down to $y = 2.5$ at 9.3 GeV. Hence, the beam and target fragmentation regions overlap to some extent at our energies. This may explain the apparent lack of a central plateau region.

FEYNMAN x VARIABLE

In terms of variables $x = p^*_{\parallel}/p^*_{max}$ and $p_\perp{}^2$ we write the differential cross section as

$$d^2\sigma = \pi \frac{p^*_{max}}{E^*} dx dp_\perp{}^2 f_3(x, p_\perp{}^2, s).$$

Feynman[2] has suggested that at high energies the structure function is independent of s, that is,

$$f_3(x, p_\perp{}^2, s) \xrightarrow[s\to\infty]{} f_3(x, p_\perp{}^2).$$

In Fig. 12 we show the integrated structure function

$$F(x) = \frac{1}{\pi}\int_0^\infty \frac{E^*}{p^*_{max}} \frac{d^2\sigma}{dx dp_\perp{}^2} dp_\perp{}^2. \quad (6)$$

The same qualitative features hold at the three energies: a rapid increase from negative x to $x = 0$ by 3 orders of magnitude, a relatively flat region to $x \sim 0.6$, and a drop at large x [the narrow peak at large x is a reflection of the Δ^{++} production via $\gamma p \to \pi^- \Delta^{++}(1236)$ which falls off rapidly

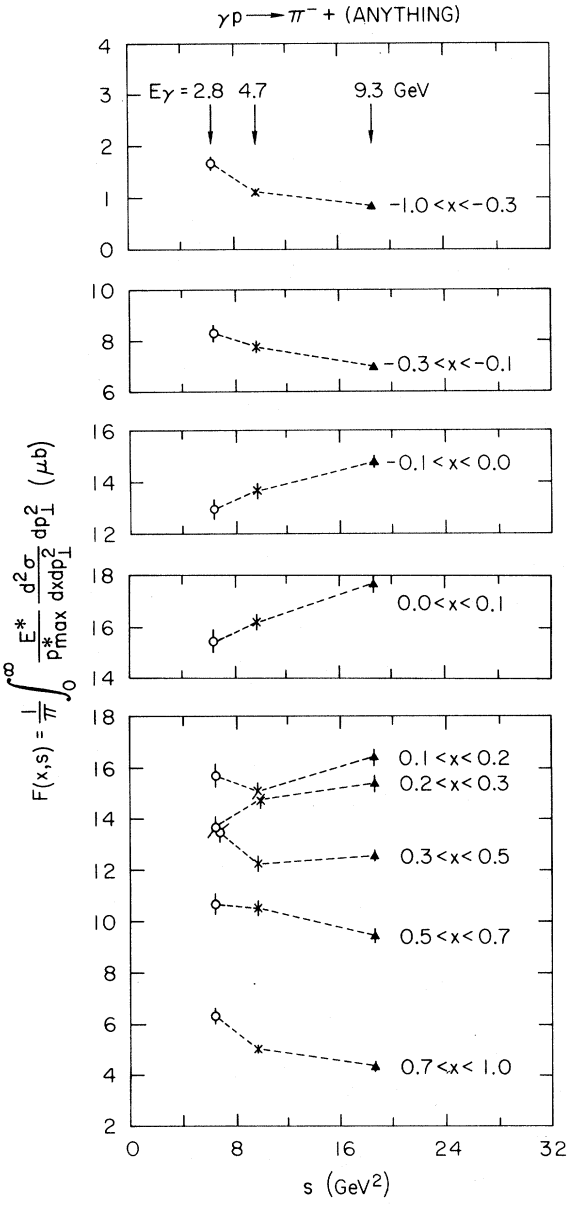

FIG. 13. The structure function $F(x,s)$ integrated over different intervals in x plotted as functions of s.

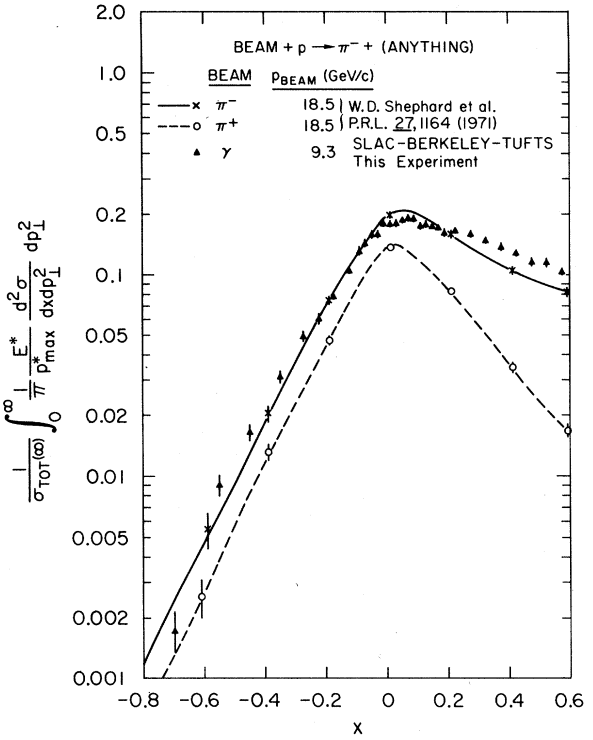

FIG. 14. Normalized structure function $F(x)/\sigma_{\text{tot}}(\infty)$ for photoproduced π^- reactions compared with those for $\pi^\pm$ induced reactions (Ref. 17). Curves are approximations to the hadron-induced data with representative data points shown.

with increasing energy]. We seem to see scaling to within ±10% over most of the x region. To investigate this apparent scaling more carefully we display the energy dependence of the integrated structure function in Fig. 13, where $F(x, s)$ is shown integrated over various x intervals as a function of s. Although, there is a tendency for the rate of change of $F(x, s)$ with respect to s to decrease, only measurements at higher energies will tell how close our 9.3-GeV data are to the scaling limit.

Figure 14 shows the comparison of the structure functions for different beam particles in terms of the x variable. We again divide our 9.3-GeV data by $\sigma_{\text{tot}}(\infty)$ and plot them together with similarly normalized $\pi^\pm$ data at 18 GeV/c of Shephard *et al.*[14,17] The region $x<0.2$ corresponds to the interval in $p_\parallel$ given in Fig. 7. Again we find that the photoproduction structure function is similar to that of $\pi^- p$ but is larger than that of $\pi^+ p$. Not unexpectedly, the shapes of the distributions do not agree for $x>0.2$, since the three reactions are initiated by different beam particles.

In the vector-dominance model (VDM) of photon interactions the reaction $\gamma p \to \rho^0 p$ can be considered the analog of elastic scattering in hadron-induced reactions. In the following we shall investigate to what extent the exclusion of this quasi-elastic process affects the behavior of the structure function.

Because of the well-known difficulties in separating ρ^0 from background[8] we have attempted to eliminate the reaction $\gamma p \to \rho^0 p$ by the simplest cut: We refer to all events of $\gamma p \to \pi^+ \pi^- p$ with $M_{\pi^+\pi^-} < 1.0$ GeV as "elastic" ρ^0 events.

In Fig. 15 we show the modified $F(x)$ after such a subtraction of "elastic" ρ^0 events as well as the

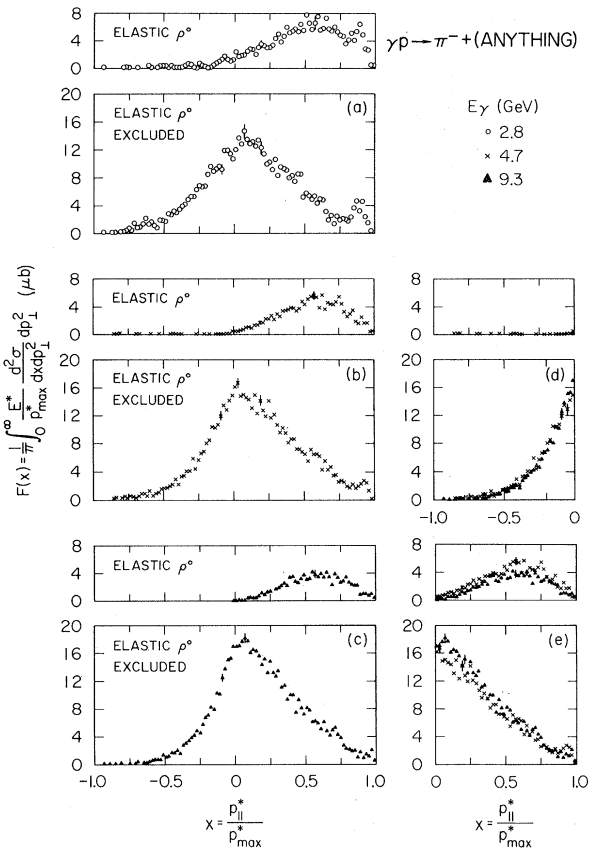

FIG. 15. $F(x)$ with the elastic ρ^0 events excluded ($\gamma p \to \pi^+\pi^- p$ with $M_{\pi^+\pi^-} < 1.0$ GeV removed), for (a) 2.8 GeV, (b) 4.7 GeV, (c) 9.3 GeV. Above each we show the contribution to $F(x)$ from the ρ^0. (d) $F(x)$ for the 4.7- and 9.3-GeV data superimposed for comparison for $x<0$. (e) Same for $x>0$.

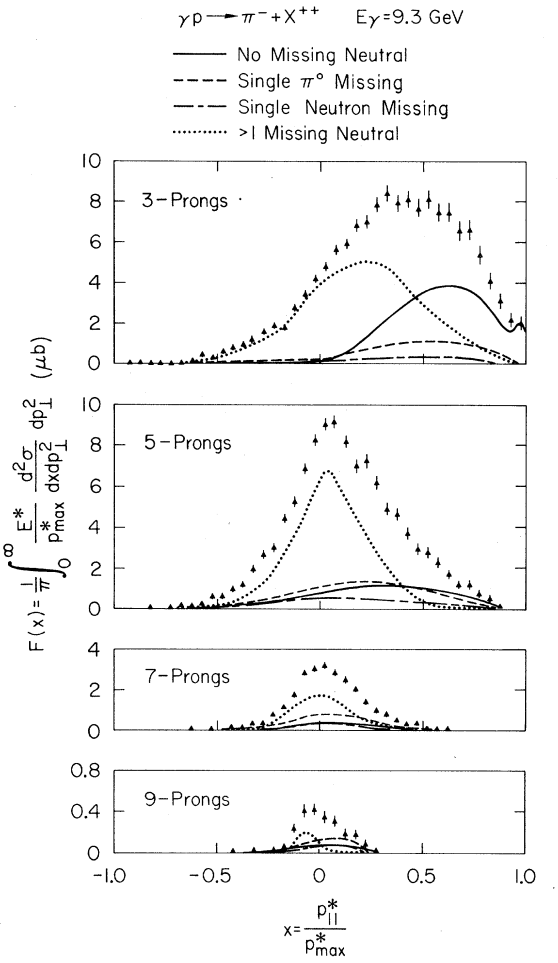

FIG. 16. $F(x)$ for 3-, 5-, 7-, 9-prong events separately at 9.3 GeV. The curves show the contributions from the events having no missing neutrals, a single π^0 missing, a single neutron missing and from multineutral events.

contribution to $F(x)$ from the eliminated events. We find that the π^- mesons from elastic ρ^0 events do not influence $F(x)$ for $x<0$. (The small contribution at 2.8 and 4.7 GeV for $x<0$ is mainly due to inclusion of background under the ρ^0 resonance; this background decreases rapidly with increasing energy.) As seen in Figs. 15(d) and 15(e) the comparison of the 4.7- and 9.3-GeV data shows that exclusion of elastic ρ^0 events does not alter our conclusions about scaling.

To explore further the composition of the structure function, we give in Fig. 16 $F(x)$ for the separate charged multiplicities at 9.3 GeV. The curves show the contributions from the events having no missing neutrals, a single π^0 missing, a single neutron missing and from multineutral events.[18] We see that almost all the contributions to $F(x)$ at large x come from 3- and 4-body production in the 3-prong events. By eliminating these events we obtain the dotted curve in Fig. 16 (top). This distribution (for five or more bodies with at least two neutrals) is somewhat similar in shape (though not in magnitude) to the 5-prong distribution which suggests that the neutral-pion distributions may be like those of the charged pions.

FACTORIZATION OF THE STRUCTURE FUNCTION

In the reaction $pp \to \pi^-$ + (anything) above 12 GeV/c, Bali *et al.*[19] found that the x and $p_\perp{}^2$ dependence of the structure function was uncoupled, i.e., they could fit the data with a factorized form for the structure function,

$$f_3(x, p_\perp{}^2) = G(x)H(p_\perp{}^2).$$

In contrast Ko and Lander[20] found in the reaction $K^+ p \to \pi^-$ + (anything) at 11.8 GeV/c that $f_3(x, p_\perp{}^2)$ did not factorize in this way. To test whether the

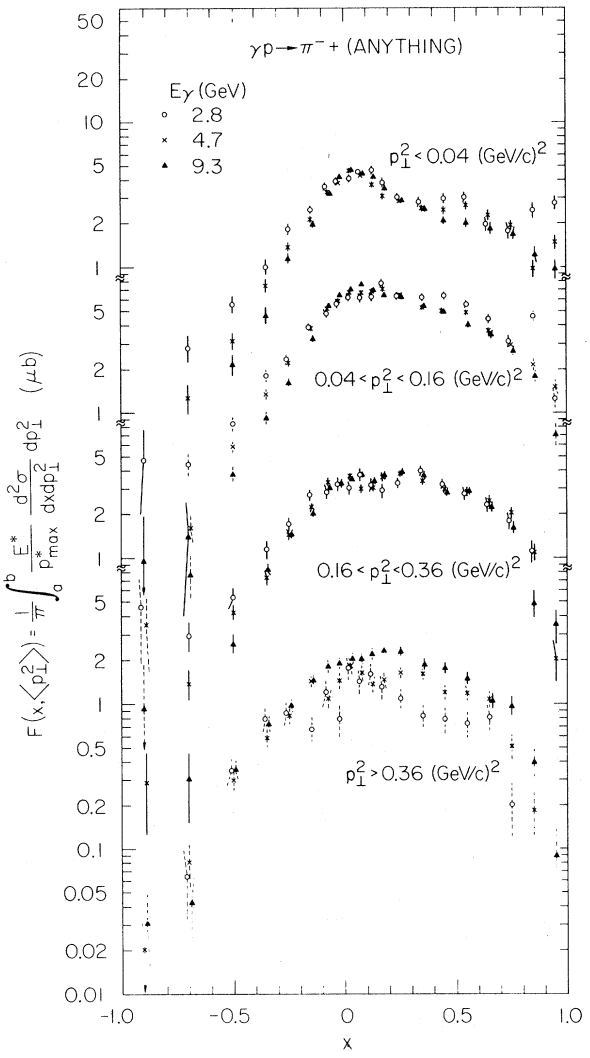

FIG. 17. The structure function $F(x,\langle p_\perp{}^2\rangle)$ plotted versus x for various intervals in transverse momentum.

structure function in $\gamma p \to \pi^- + (\text{anything})$ may be factorized we give in Fig. 17 plots of

$$F(x,\langle p_\perp{}^2\rangle)=\frac{1}{\pi}\int_a^b \frac{E^*}{p^*_{\max}}\frac{d^2\sigma}{dx\,dp_\perp{}^2}\,dp_\perp{}^2,$$

where a and b are the limits of the various $p_\perp{}^2$ intervals shown. The distributions in $F(x,\langle p_\perp{}^2\rangle)$ do not have the same shape for all intervals of $p_\perp{}^2$, i.e., the structure function does not factorize This is also seen in Fig. 18 where we display

$$f_3(x,p_\perp{}^2)=\frac{1}{\pi}\frac{E^*}{p^*_{\max}}\frac{\Delta^2\sigma}{\Delta x\,\Delta p_\perp{}^2}$$

for the different x intervals indicated.

The quantitative changes in the $p_\perp{}^2$ dependence of the structure functions are more clearly seen in Fig. 18(b) where three x regions are shown in an expanded scale. The exponential decrease of $f_3(x,p_\perp{}^2)$ with $p_\perp{}^2$ is faster near $x=0$ than for other x intervals. Yen and Berger[21] and Berger and Krzywicki[22] have suggested that the increase in the concentration of pions at small x and $p_\perp{}^2$ is due to generation of pions which are decay products of resonances [e.g., $\Delta(1236)$, $N^*(1680)$] with small Q values.

From Fig. 18(b) we also see $f_3(x,p_\perp{}^2)$ flattens for the x interval $0.3<x<0.5$ at small $p_\perp{}^2$ which is due to elastic ρ^0 events and their peripheral production mechanism and decay ($\sin^2\theta$ in the helicity system) into $\pi^+\pi^-$.[8]

We now turn to a comparison of the structure function for different charge multiplicities. Friedman[23] and Berger and Krzywicki[22] have pointed out that there is a phase-space effect: As the multiplicity increases the dimensionality of phase space increases favoring pions at smaller c.m. momenta. This causes a more rapid falloff both in x (as seen in Fig. 16) and $p_\perp{}^2$. Therefore, we would expect the structure function for higher charged multiplicities (more prongs) to show a steeper falloff in $p_\perp{}^2$ at any x. The same is expected for higher neutral multiplicities. Since we cannot separate events with different numbers of neutral particles, this effect will cause a steepening of the $p_\perp{}^2$ distribution of the π^- mesons at small $|x|$ for a given charged multiplicity.

In Fig. 19 we show that the transverse-momentum dependence changes with x at a given multiplicity. The straight lines are exponential fits to the data for $p_\perp{}^2<0.3$ $(\text{GeV}/c)^2$. The exponential slope A from these fits is given in Table I. There is a steeper falloff in $p_\perp{}^2$(as seen by larger values of A) as the multiplicity increases. Also, at a fixed multiplicity the falloff is steeper in the interval $-0.1<x<0.1$ than for other x regions. Thus our data seem to support the kinematic argument.

AVERAGE π^- MULTIPLICITY AND SCALING

Scaling predicts that at sufficiently high energy the π^- multiplicity $\langle n^-\rangle$ will obey the relation

$$\langle n^-\rangle = c^- \ln s + d^-, \qquad (7)$$

where c^- and d^- are energy-independent.[19, 24] It is interesting to investigate how well this form de-

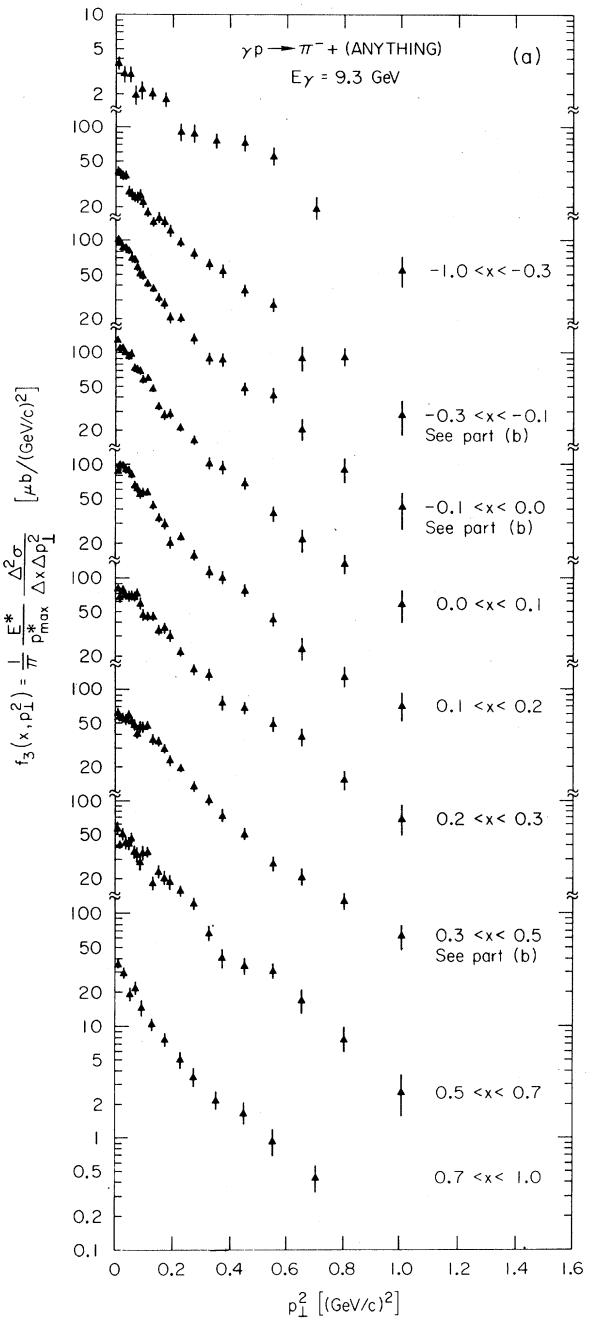

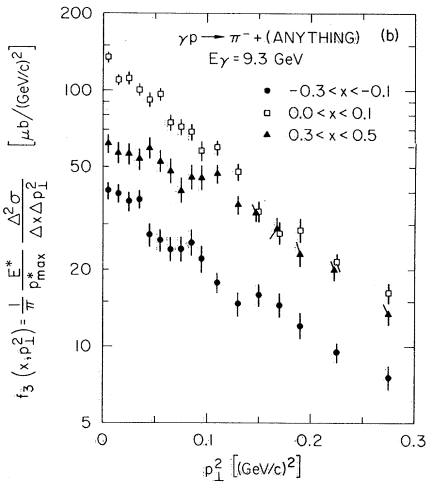

FIG. 18. Structure function $f_3(x,p_\perp^2)$ at 9.3 GeV (a) for finite x intervals. (b) Same data for selected x intervals shown on an expanded scale.

scribes the data at our finite energies. In Fig. 20 we show the average charged-prong and π^- multiplicities for our four photon energies. For $\langle n^-\rangle$ we find the form of Eq. (7) fits well with $c^- = 0.44 \pm 0.04$ and $d^- = 0.07 \pm 0.08$ (for s in GeV^2). However, we also find the dependence of $\langle n^-\rangle$ on s is compatible with a power-law behavior.

Following Bali *et al.*[19] we can approximately calculate c^- from the structure function. The average π^- multiplicity is

$$\langle n^-\rangle = \frac{\sum n^-\sigma_{n^-}}{\sigma_{tot}},$$

where σ_{n^-} is the topological cross section for production of n^- negative pions. Then, because the inclusive cross section, $d^2\sigma$, counts the production of n^- negative pions n^- times, $\sum n^-\sigma_{n^-} = \int\int d^2\sigma$ and

$$\langle n^-\rangle = \frac{\pi}{\sigma_{tot}} \int\int dx dp_\perp{}^2 \frac{f_3(x,p_\perp{}^2)}{[x^2 + (p_\perp{}^2+\mu^2)/p^{*2}_{max}]^{1/2}},$$

where μ is the pion mass. Expanding f_3 about $x=0$, we find[24]

$$\langle n^-\rangle = \frac{\pi}{\sigma_{tot}}\left[\int_0^\infty dp_\perp{}^2 f_3(0,p_\perp{}^2)\right] \ln s + \text{const} + O(s^{-1}\ln s), \quad (8)$$

where we have used the approximation $p^*_{max} \simeq \frac{1}{2}\sqrt{s}$. For our data the quantity in brackets is just $F(0)$ which is plotted in Fig. 12 and is 14.7 ± 1.0, 16.0 ± 0.7, and 17.1 ± 0.7 μb at 2.8, 4.7, and 9.3 GeV [a small correction <1.3% has been applied to correct $F(0)$ for the strange-particle events]. Using for σ_{tot} our values of 133 ± 3, 127 ± 3, and 122 ± 4 μb, we find for the coefficient of ln$s$ values of 0.35 ± 0.03, 0.40 ± 0.02, and 0.44 ± 0.02 at 2.8, 4.7, and 9.3 GeV which are similar to the slope $c^- = (0.44 \pm 0.04)$ found from the fit to the measured π^- multiplicity. The increase of c^- with increasing energy is caused by the decrease of the total cross section (~4% between energies) and the increase of the integrated structure function at $x=0$ (~7% between energies). It is interesting that the

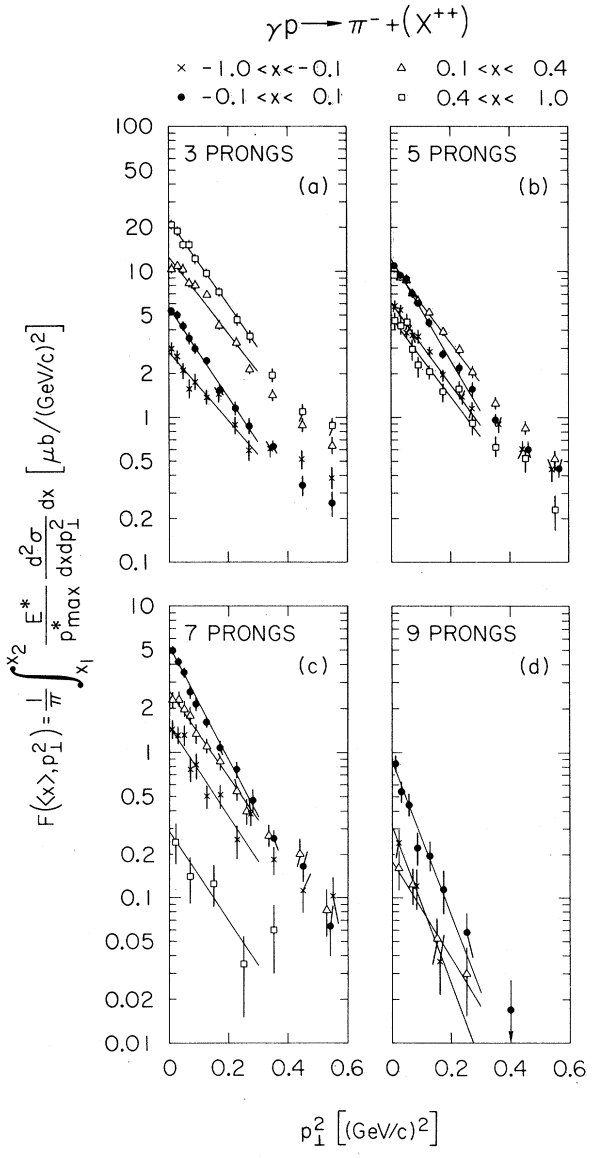

FIG. 19. $F(\langle x\rangle, p_\perp^2)$ for 3-, 5-, 7-, 9-prong events separately at 9.3 GeV. The curves are the results of fits to $F(\langle x\rangle, 0)\exp(-Ap_\perp^2)$ for $p_\perp^2 < 0.3$ $(\text{GeV}/c)^2$. See Table I for values of A.

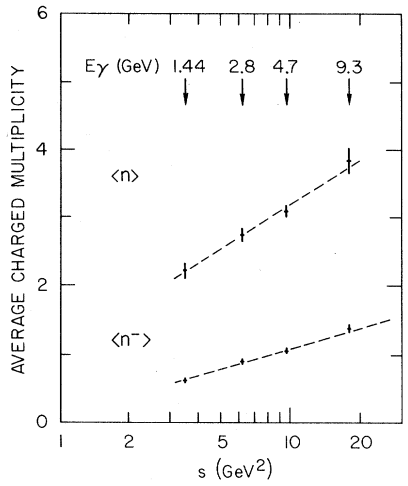

FIG. 20. Average charged-prong multiplicity (labeled $\langle n\rangle$) and π^- (labeled $\langle n^-\rangle$) versus s. The straight lines are the results of a fit of the data to the form $\langle n\rangle = c\ln s + d$ ($c = 0.93 \pm 0.12$, $d = 1.01 \pm 0.22$) and ($c^- = 0.44 \pm 0.04$, $d^- = 0.07 \pm 0.08$).

approximations used in deriving Eq. (8) seem to be quite good at our moderate energies.

We remark that any reasonably smooth scaling distribution in x and $p_\perp^2$ results at very high energy in a y distribution having limiting fragmentation and a flat region in $d\sigma/dy$ [in fact, if $f_3(x, p_\perp^2)$ exhibits scaling for all incident particles, properties (i), (ii), and (iii) previously mentioned in the section on the rapidity variable will follow]. In particular, a flat plateau in $d\sigma/dy$ (presumably indicating pionization) is predicted [a fixed interval in x of width ϵ about $x = 0$ transforms into a region in y of width $\ln(s\epsilon^2)$ and height $\pi F(x = 0)$]. Alternatively, a flat region in $d\sigma/dy$ would lead to a $\ln s$ increase of the average multiplicity $\langle n^-\rangle$ and scaling in x. However, at our relatively low photon energies no clear flat region in $d\sigma/dy$ is seen (Fig. 10). Nevertheless, the integral of

$$\frac{1}{\sigma_{\text{tot}}}\frac{d\sigma}{dy}$$

is increasing as $\ln s$ thus giving $\langle n^-\rangle \propto \ln s$. This

TABLE I. Values of the exponential slope A $[(\text{GeV}/c)^{-2}]$ fitting the structure function $F(\langle x\rangle, p_\perp^2)$ of Fig. 19 for $p_\perp^2 < 0.3$ $(\text{GeV}/c)^2$ to $F(\langle x\rangle, p_\perp^2) = F(\langle x\rangle, 0)\exp(-Ap_\perp^2)$. Data at 9.3 GeV.

x	3-prongs [a]	5-prongs [a]	7-prongs [a]	9-prongs [a]
(−1.0)−(−0.1)	5.3 ± 0.5	6.4 ± 0.4	7.2 ± 0.9	12.5 ± 4.3
(−0.1)−(0.1)	7.3 ± 0.3	7.9 ± 0.3	9.2 ± 0.4	11.9 ± 1.5
(0.1)−(0.4)	6.0 ± 0.3	6.1 ± 0.3	6.8 ± 0.6	7.8 ± 2.4
(0.4)−(1.0)	6.8 ± 0.3	6.2 ± 0.6	7.2 ± 2.9	...

[a] An N-prong event has N charged particles without detected strange-particle decay.

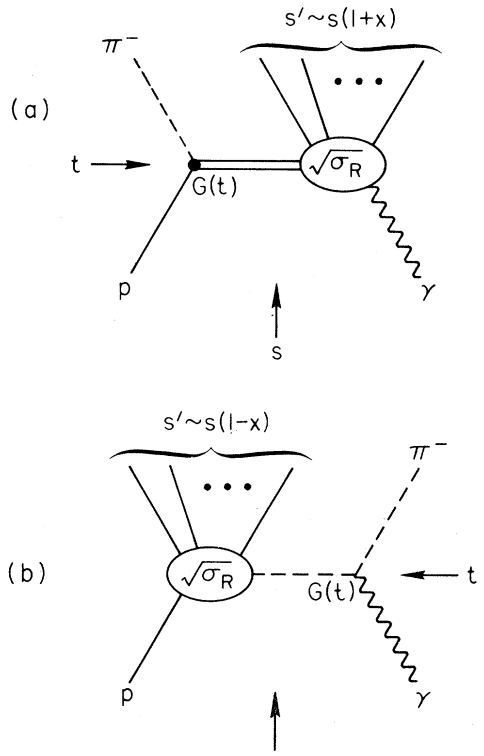

FIG. 21. Dominant diagram expected to contribute to π^- production near the kinematic boundaries for (a) target-associated π^- and (b) beam-associated π^-.

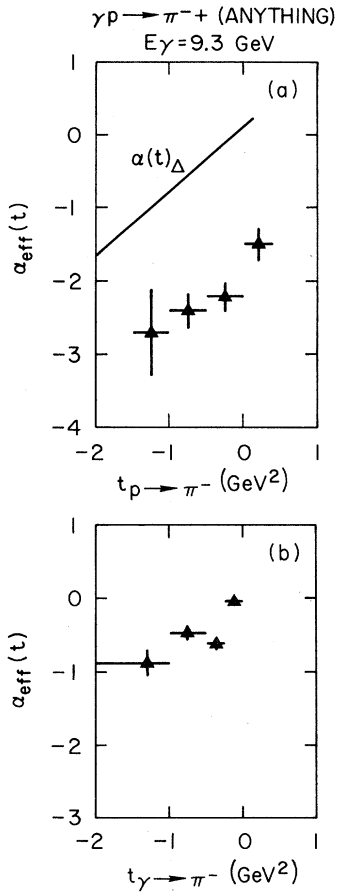

FIG. 22. Values of the effective Regge trajectory, determined as described in the text, as a function of t for (a) target vertex and (b) photon vertex. The curve corresponds to the Δ trajectory.

behavior is unrelated to an extended flat region and thus from our data we are unable to establish pionization as the mechanism responsible for the increase of $\langle n^- \rangle$.

REGGE TRAJECTORIES AND THE STRUCTURE FUNCTION

Feynman has suggested[2] that if scaling occurs, then, at the extremes of x one should have

$$f(x, t) = (1 - |x|)^{1-2\alpha(t)}, \tag{9}$$

where $\alpha(t)$ is the highest Regge trajectory that could carry off the quantum numbers and momentum transfer at the $\gamma \to \pi$ (at $x = 1$) and $p \to \pi$ ($x = -1$) vertices. Such behavior can also be predicted by the multiperipheral model. Caneschi and Pignotti[25] using a multi-Regge model for the part of the cross section due to the diagrams of Fig. 21 have obtained the following expression (in the limit of large s, large missing mass squared, s', and large ratio s/s'):

$$\frac{d^3\sigma}{d^3p} = \frac{1}{E}\left(\frac{s}{s'}\right)^{2\alpha(t)-1} |G(t)|^2 \sigma_R^{\text{tot}}(s', t). \tag{10}$$

Here $\alpha(t)$ is the Regge trajectory exchanged, which is coupled to the proton (photon) with a residue function $G(t)$. $\sigma_R^{\text{tot}}(s', t)$ is to be interpreted as a Reggeon-photon (proton) total cross section. Now, in terms of the c.m. energy E^* of the outgoing π^-,

$$\frac{s'}{s} = \frac{\mu^2}{s} + 1 - \frac{2E^*}{\sqrt{s}} \sim 1 - |x|,$$

for s large and $p_\parallel{}^2 \gg p_\perp{}^2 + \mu^2$. If we assume $\sigma_R^{\text{tot}}(s', t)$ to be asymptotically constant in s', we obtain Eq. (9) after equating

$$f(x, t) = E\frac{d^3\sigma}{d^3p}.$$

We have determined $\alpha(t)$ in Eq. (10) by fitting the experimental distribution for our 9.3-GeV data to $(s'/s)^{1-2\alpha(t)}$ for finite t intervals. We fitted over two ranges: $a < s'/s < 0.7$ for the target region and $b < s'/s < 0.5$ for the beam region. The limits $a \sim 0.25$ and $b \sim 0.1$ were adjusted for each t interval to avoid effects due to the kinematic boundary in (s'/s) and t. While $s = 18.3$ GeV^2 may be considered large, we recognize that the lower limits, $s' = 1.8$ GeV^2 and $(s/s') = 1.4$ are not large as was required in the derivation of Eq. (10).

In Fig. 22(a) we give resulting values of $\alpha(t)$ for the $p \to \pi$ vertex [target region and diagram of Fig. 21(a)]. The values of $\alpha(t)$ are much lower than the known leading Regge trajectory (Δ in this case)[26] but similar to those obtained from other inclusive experiments,[27,28] e.g., $pp \to \pi^- + (\text{anything})$. Discussion of this discrepancy can be found in Refs. 27 and 28.

In Fig. 22(b) we give $\alpha(t)$ for the $\gamma \to \pi$ vertex. (Elastic ρ^0 events have been included.) Here the $\alpha(t)$ is compatible with a Regge trajectory of slope 1 GeV^{-2} and $\alpha(0)=0$; from VDM we would expect this trajectory to be associated with the pion.

POLARIZATION DEPENDENCE

Next we look for a correlation between the azimuthal angle ϕ of the π^- and the polarization vector ϵ of the photon: 93%, 91%, and 77% average polarization at 2.8, 4.7, and 9.3 GeV. We define ϕ as

$$\phi = \tan^{-1}\left(\frac{\hat{k}\times\hat{\epsilon}\cdot\vec{p}_\perp}{\hat{\epsilon}\cdot\vec{p}_\perp}\right),$$

where $\hat{k}$ is a unit vector in the direction of the incident photon. In Fig. 23 we show for the 9.3-GeV data

$$\frac{d\sigma}{d\phi} = \frac{1}{\pi}\int_{x_1}^{x_2} dx \int_0^\infty dp_\perp{}^2 \frac{E^*}{p^*_{\max}} \frac{d^3\sigma}{dx\,dp_\perp{}^2\,d\phi}$$

for various x intervals. Here, the elastic ρ^0 production events and the residual events are shown separately. A fit to the data to the form $d\sigma/d\phi = A + B\cos^2\phi$ results in values for A and B given in Table II for the three energies (no correction has been applied to account for the unpolarized component in the beam). We find no statistically significant correlation between the π^- and the polarization vector for $x<0.3$. However, some correlation is present for $x>0.3$. On the other hand, even for $x>0$ elastic ρ^0 events show a strong correlation. The lack of correlation of the π^- with the polarization vector for $x<0.0$ is consistent with factorization (in the Regge sense) of the residues of the photon and target vertices.[29]

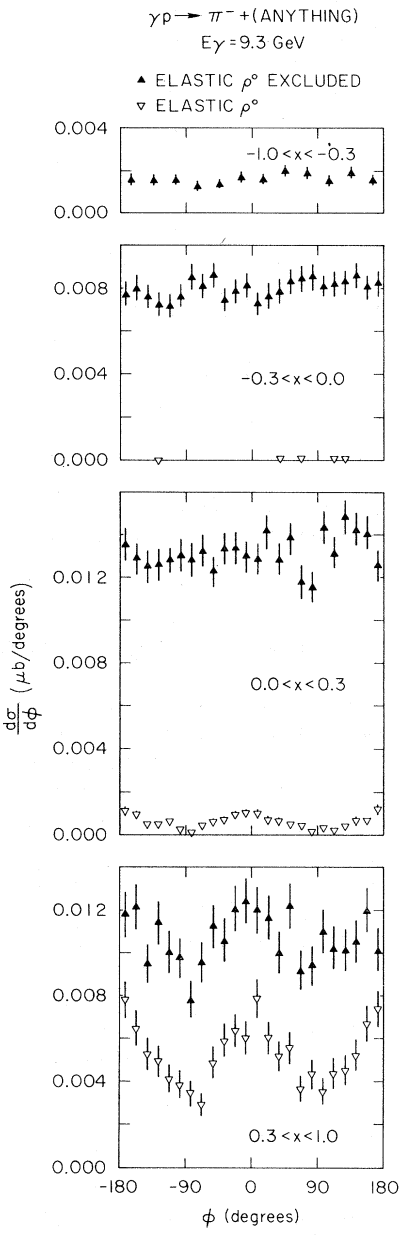

FIG. 23. The differential cross section $d\sigma/d\phi$ plotted against the azimuthal angle ϕ between the outgoing pion and the polarization vector of the photon, for various x intervals. Elastic ρ^0 production is not included in the ▲ points and is given separately by the ▽ points. Data are at 9.3 GeV.

LORENTZ FRAME FOR A SYMMETRIC LONGITUDINAL-MOMENTUM DISTRIBUTION

The $F(x)$ distributions showed an asymmetry about $x=0$ (see Figs. 12 and 15) which has also been found in inclusive $\pi^- p$ studies. In the case of $\pi^- p$ reactions, Elbert *et al.*[30] studied the composite $p_{\parallel}$ distribution in the c.m. system of backward π^- and forward π^+ and found that by Lorentz transforming to a frame where the ratio R of the incident proton momentum to the incident π^- momentum is 1.5 (the "Q system" in their notation), the longitudinal-momentum distribution of the π becomes symmetric. This result has been interpreted in the framework of the quark model. If there are two quarks in the π and three quarks in the proton, in this "quark" frame all five quarks have the same average value of $|p|$. Thus, in this interpretation the symmetric distribution for $R=1.5$ results from symmetry in the quark-quark

TABLE II. Value of A and B fitting $d\sigma/d\phi$ to the form $d\sigma/d\phi = (A + B\cos^2\phi)$.

E_γ (GeV)	x	Elastic ρ^0 excluded [a]		Elastic ρ^0 only [a]	
		A (nb/deg)	B (nb/deg)	A (nb/deg)	B (nb/deg)
2.8	(−1.0)−(−0.3)	2.80±0.22	0.24±0.37	0.24±0.08	0.07±0.13
	(−0.3)−(0.0)	7.36±0.29	0.17±0.47	0.29±0.06	0.28±0.11
	(0.0)−(0.3)	9.65±0.33	0.73±0.55	0.89±0.12	2.65±0.25
	(0.3)−(1.0)	7.60±0.39	2.24±0.66	7.06±0.41	5.42±0.73
4.7	(−1.0)−(−0.3)	2.16±0.14	−0.18±0.22	0.04±0.03	0.05±0.05
	(−0.3)−(0.0)	7.82±0.21	0.22±0.36	0.04±0.02	0.00±0.02
	(0.0)−(0.3)	11.51±0.25	−0.05±0.41	0.43±0.06	1.40±0.13
	(0.3)−(1.0)	8.38±0.30	2.61±0.52	4.30±0.25	5.21±0.46
9.3 [b]	(−1.0)−(−0.3)	1.55±0.12	0.08±0.20	...	...
	(−0.3)−(0.0)	7.95±0.19	−0.03±0.30	...	...
	(0.0)−(0.3)	12.87±0.25	0.45±0.42	0.21±0.04	0.77±0.08
	(0.3)−(1.0)	9.48±0.33	2.29±0.56	3.41±0.22	3.53±0.41

[a] Elastic ρ^0 event: $\gamma p \to \pi^-\pi^+ p$ with $M_{\pi^+\pi^-} < 1.0$ GeV.
[b] Data plotted in Fig. 23.

center-of-mass system for the quark-quark collision that takes place.

In Fig. 24 we show the $p_\parallel$ distribution for the 9.3-GeV photon data in the frames where $R = 1.0$, 1.5, and 2.3. $R = 2.3$ yields a symmetric distribution. Here we have excluded elastic ρ^0 production as before. Table III gives the values of R needed to obtain symmetry at our three energies. We also determined the symmetric frame with elastic ρ^0 events included and Table III shows even larger values of R (~3) in this case. We conclude that the Q system does not give symmetry for photoproduced π^-. In the spirit of the Q-system argument, a value of $R = 3$ would suggest that the photon interacts as a *single* quarklike object with one of the three quarks of the proton.

CONCLUSIONS

(1) We find a decrease of $E\,d\sigma/dp_\parallel$ in the target region ($p_\parallel < 300$ MeV) with increasing photon energy. Thus limiting target fragmentation in the strict sense of Ref. 1 is not observed. The energy dependence of $E\,d\sigma/dp_\parallel$ is compatible with approaching a limiting distribution as $A + Bs^{-1/2}$ as predicted by Chan *et al.*[12] (Figs. 4 and 6).

(2) We observe a significant decrease in $d\sigma/dy$ with increasing photon energy both in the target and beam fragmentation regions. For the central region of the "rapidity" distribution no extended flat region is observed (Fig. 10).

(3) The qualitative features of the structure function in terms of Feynman's x variable are similar for all x at the three energies. There are, however, small but statistically significant differences between the three energies (Figs. 12 and 13).

(4) We find that the structure function $f_3(x, p_\perp^2)$ does not factorize into independent functions of x and $p_\perp^2$ (Figs. 17 and 18).

(5) Even at our moderate photon energies (1.4 to 9.3 GeV) the increase in π^- multiplicity is consistent with a logarithmic growth in s (Fig. 20).

(6) When interpreted in a Regge framework, the t dependence of the structure function leads to a trajectory associated with the $\gamma \to \pi^-$ vertex (forward π^- production) with $\alpha(0) \approx 0.0$ and a slope ≈ 1 GeV^{-2}; for the trajectory associated with the $p \to \pi^-$ vertex (backward π^- production) one obtains a similar slope but an $\alpha(0)$ which is lower than that of the expected leading trajectory (the Δ) (Fig. 22).

(7) There is no azimuthal correlation of the outgoing π^- and the polarization vector of the incident photon for $x < 0$. For $x > 0$ we find a significant correlation approximately half of which comes from elastic ρ^0 production (Fig. 23 and Table II).

(8) The Q system of Elbert *et al.*,[30] does not result in a symmetric distribution in $p_\parallel$ for the

TABLE III. Value of $R = p_{\text{proton}}/p_{\text{photon}}$ for the frame in which the π^- longitudinal-momentum distribution is symmetric.

E_γ (GeV)	R	
	Elastic ρ^0 excluded [a]	Elastic ρ^0 included [a]
2.8	1.75±0.05	2.95±0.1
4.7	1.85±0.05	2.75±0.1
9.3	2.3 ±0.05	2.75±0.1

[a] Elastic ρ^0 event: $\gamma p \to \pi^+\pi^- p$ with $M_{\pi^+\pi^-} < 1.0$ GeV.

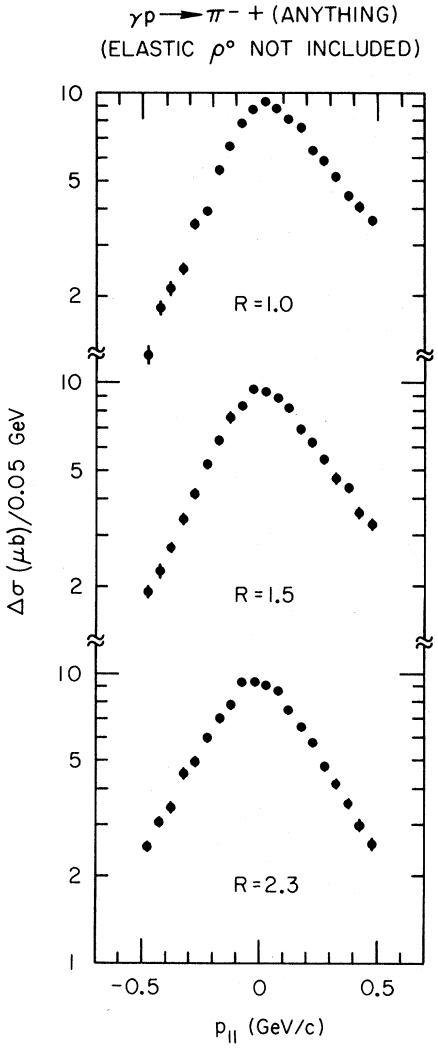

FIG. 24. The longitudinal-momentum $p_\parallel$ distributions at 9.3 GeV in the frame where $R = p_{\text{proton}}/p_{\text{photon}}$ has the value (a) $R = 1.0$ (c.m. frame), (b) $R = 1.5$ (Q system), and (c) $R = 2.3$ (symmetric frame). Elastic ρ^0 production events have been excluded.

π^-. We find at 9.3 GeV that symmetry is reached for the ratio of colliding momenta $R = 2.3$ with elastic ρ^0 removed and $R = 2.75$ with elastic ρ^0 included (Fig. 24 and Table III).

(9) When scaled by the total cross section our inclusive π^- cross sections in the target region are similar to those found in $\pi^- p$ reactions. They are larger by a factor of ≈ 2 than those obtained from $\pi^+ p$, $K^+ p$, and pp reactions (Figs. 7 and 14).

ACKNOWLEDGMENTS

We acknowledge the stimulating discussions we have had with Professor J. D. Bjorken, Professor H. Abarbanel, and Dr. C. Risk. We wish to thank the SLAC operations crew of the accelerator and R. Watt and the 82-in. bubble-chamber operation group. The diligent work of the scanners at SLAC and Berkeley is gratefully acknowledged. We gratefully acknowledge the contribution of W. R. Graves, Dr. Jim Murray, and Dr. G. Smadja.

*Work supported in part by the U. S. Atomic Energy Commission and the National Science Foundation.

†On leave from College de France, Paris, France.

‡On leave from Max-Planck Institut für Physik und Astrophysik, Munich, Germany.

§Present address: University of Glasgow, Department of Natural Philosophy, Glasgow, Scotland.

‖On leave from University of Hamburg, Hamburg, Germany.

**Present address: DESY, Hamburg, Germany.

††Present address: Laboratoire Interuniversitaire des Hautes Energies, Brussels, Belgium.

[1]J. Benecke, T. T. Chou, C. N. Yang, and E. Yen, Phys. Rev. 188, 2159 (1969).

[2]R. P. Feynman, Phys. Rev. Letters 23, 1415 (1969); California Institute of Technology report, 1969 (unpublished); see also *High Energy Collisions*, Third International Conference held at State University of New York, Stony Brook, 1969, edited by C. N. Yang *et al.* (Gordon and Breach, New York, 1969), p. 237.

[3]K. G. Wilson, Acta Phys. Austr. 17, 37 (1963); Cornell Report No. CLNS-131, 1970 (unpublished).

[4]Carleton E. DeTar, Phys. Rev. D 3, 128 (1971). The literature concerning multiperipheral models and their predictions for the inclusive reactions can be traced from this publication.

[5]As suggested by Feynman (private communication) we use $x = p_\parallel^*/p_{\max}^*$ with $-1 \le x \le 1$ at our finite energies

instead of the asymptotic form $x = 2p_{\parallel}^{*}/\sqrt{s}$ given in Ref. 2.

[6]J. C. Vander Velde, Phys. Letters 32B, 501 (1970).

[7]The cross section per event for the inclusive π^- distributions was obtained directly from the photon flux (see Ref. 8). To account for the negative pions in the strange-particle events a correction should be made to these distributions as we have done for Figs. 7 and 14 where we compare our data with hadron-induced reactions.

[8]J. Ballam, G. B. Chadwick, R. Gearhart, Z. G. T. Guiragossián, P. R. Klein, A. Levy, M. Menke, J. J. Murray, P. Seyboth, G. Wolf, C. K. Sinclair, H. H. Bingham, W. B. Fretter, K. C. Moffeit, W. J. Podolsky, M. S. Rabin, A. H. Rosenfeld, and R. Windmolders, Phys. Rev. Letters 23, 498 (1969); 23, 817(E) (1969); M. Rabin *et al.*, Bull. Am. Phys. Soc. 15, 1634 (1970). For other experimental details and results of this experiment see H. H. Bingham *et al.*, Phys. Rev. Letters 24, 955 (1970); J. Ballam *et al.*, *ibid.* 24, 960 (1970); 24, 1467(E) (1970); also, Phys. Rev. D 5, 545 (1972).

[9]For example, see D. B. Smith *et al.*, Phys. Rev. Letters 23, 1064 (1969).

[10]See also W. P. Swanson, M. Davier, I. Derado, D. C. Fries, F. F. Liu, R. F. Mozley, A. Odian, J. Park, F. Villa, and D. Yount, Phys. Rev. Letters 27, 1472 (1971). These authors used the SLAC streamer chamber and a bremsstrahlung photon beam with photon energies from 5 to 18 GeV and report a similar energy dependence for $d\sigma/dp_{\parallel}$ in the region $p_{\parallel} < 500$ MeV/c.

[11]A. H. Mueller, Phys. Rev. D 2, 2963 (1970).

[12]Chan Hong-Mo, C. Hsue, C. Quigg, and Jiunn-Ming Wang, Phys. Rev. Letters 26, 672 (1971).

[13]M.-S. Chen, R. R. Kinsey, T. W. Morris, R. S. Panvini, L.-L. Wang, T. F. Wong, S. L. Stone, T. Ferbel, P. Slattery, B. Werner, J. W. Elbert, and A. R. Erwin, Phys. Rev. Letters 26, 1585 (1971).

[14]For the asymptotic values of the total cross sections, Chen *et al.* (Ref. 13) use 23.4, 17.4, 39.8, and 24.9 mb for $\pi^+ p$, $K^+ p$, pp, and $\pi^- p$ incident channels, respectively. For γp we use $\sigma_{\rm tot}(\infty) = 99$ μb which results from a fit to the form $\sigma_{\rm tot}(s) = a + Bs^{-1/2}$ by Hesse *et al.* (Ref. 15) Corrections were also applied to the γp data to account for the π^- production in the strange-particle topologies.

[15]W. P. Hesse, D. O. Caldwell, V. B. Elings, R. J. Morrison, F. V. Murphy, B. W. Worster, and D. E. Yount, Phys. Rev. Letters 25, 613 (1970).

[16]We know of no experiment that has shown a flat distribution in y. The Echo Lake experiment shows distributions in $\log_{10}\tan\theta_{\rm lab}$ which for $p_{\parallel} \gg p_{\perp} \gg M_{\pi}$ is related to y [$y \simeq \ln(2/\tan\theta_{\rm lab})$]; they obtain distributions which show no clear flat central region at energies 146 and 211 GeV. L. W. Jones *et al.*, Phys. Rev. Letters 25, 1679 (1970); D. E. Lyon, Jr. *et al.*, *ibid.* 26, 728 (1971).

[17]W. D. Shephard, J. T. Powers, N. N. Biswas, N. M. Cason, V. P. Kenney, R. R. Riley, D. W. Thomas, J. W. Elbert, and A. R. Erwin, Phys. Rev. Letters 27, 1164 (1971); 28, 260(E) (1972).

[18]The curves for final states with a single π^0 or neutron were obtained from all events with an appropriate zero-constraint "fit" with neutral missing mass squared MM^2 in the regions $-0.08 < (\mathrm{MM})^2 < 0.12$ GeV^2 and $0.65 < (\mathrm{MM})^2 < 1.1$ GeV^2, respectively. No further cuts or corrections were applied.

[19]N. F. Bali, L. S. Brown, R. D. Peccei, and A. Pignotti, Phys. Rev. Letters 25, 557 (1970). Because the experimental pp data used was limited to x values $\gtrsim 0.05$, this work did not test the factorization hypothesis at $x \simeq 0$ where the $K^+ p$ (see Ref. 20) and γp (this experiment) data have the greatest change of the structure function dependence on transverse momentum.

[20]W. Ko and R. L. Lander, Phys. Rev. Letters 26, 1064 (1971); 28, 260(E) (1972).

[21]Edward Yen and Edmond L. Berger, Phys. Rev. Letters 24, 695 (1970).

[22]Edmond L. Berger and A. Krzywicki, Phys. Letters 36B, 380 (1971).

[23]J. Friedman (private communication).

[24]Here we briefly rederive the results of Bali *et al.* (Ref. 19) giving Eq. (8). At high energies, the contribution to the integral

$$\langle n^- \rangle = \frac{\pi}{\sigma_{\rm tot}} \int_0^\infty dp_\perp{}^2 \int_{-1}^{1} dx \, \frac{f_3(x, p_\perp{}^2)}{[x^2 + (p_\perp{}^2 + \mu^2)/p_{\rm max}^{*\,2}]^{1/2}}$$

comes mainly from the vicinity of $x = 0$. For convenience let

$$a \equiv \frac{(p_\perp{}^2 + \mu^2)^{1/2}}{p_{\rm max}^{*}}, \quad f = f_3(0, p_\perp{}^2), \quad f' = \left.\frac{\partial f_3}{\partial x}\right|_{x=0}, \quad \text{etc.}$$

After expanding $f_3(x, p_\perp{}^2)$ about $x = 0$,

$$f_3(x, p_\perp{}^2) = f + xf' + \tfrac{1}{2}x^2 f'' + \cdots,$$

we find

$$\begin{aligned}
\int_{-1}^{1} dx \, \frac{f_3(x, p_\perp{}^2)}{(x^2 + a^2)^{1/2}} &= f \int_{-1}^{1} \frac{dx}{(x^2 + a^2)^{1/2}} + f' \int_{-1}^{1} \frac{x\,dx}{(x^2 + a^2)^{1/2}} \\
&\quad + \tfrac{1}{2} f'' \int_{-1}^{1} \frac{x^2 dx}{(x^2 + a^2)^{1/2}} + \cdots \\
&= 2(f - \tfrac{1}{4}a^2 f'') \ln\left(\frac{1 + (1 + a^2)^{1/2}}{a}\right) \\
&\quad + \tfrac{1}{2} f'' (1 + a^2)^{1/2} + \cdots \\
&\underset{s \to \infty}{\sim} \left(f - \frac{(p_\perp{}^2 + \mu^2)}{s} f''\right) \ln\left(\frac{s}{p_\perp{}^2 + \mu^2}\right) \\
&\quad + \tfrac{1}{2} f'' \left(1 + 2\,\frac{(p_\perp{}^2 + \mu^2)}{s}\right) + \cdots,
\end{aligned}$$

where we have used $p_{\rm max}^{*} \sim \frac{1}{2}\sqrt{s}$. Integrating over $dp_\perp{}^2$, we find

$$\langle n^- \rangle = \left(\frac{\pi}{\sigma_{\rm tot}} \int_0^\infty dp_\perp{}^2 f_3(0, p_\perp{}^2)\right) \ln s + \text{const} + O(s^{-1} \ln s)$$

provided that (i) $f_3(x, p_\perp{}^2)$ scales and reaches a nonzero limit at $x = 0$, (ii) the integral over $dp_\perp{}^2$ converges, i.e., the distribution in $p_\perp{}^2$ is limited, e.g., as $\exp(-Ap_\perp{}^2)$, and (iii) the total cross section is asymptotically finite.

[25]L. Caneschi and A. Pignotti, Phys. Rev. Letters 22, 1219 (1969).

[26]V. D. Barger and D. B. Cline, *Phenomenological Theories of High Energy Scattering* (Benjamin, New York, 1969), p. 126.

[27]R. D. Peccei and A. Pignotti, Phys. Rev. Letters 26, 1076 (1971).

[28]Clifford Risk, LRL Report No. UCRL-20841, 1971 (unpublished).
[29]H. Abarbanel and D. Gross, Phys. Rev. Letters 26, 732 (1971).
[30]J. Elbert, A. R. Erwin, and W. D. Walker, Phys. Rev. D 3, 2042 (1971).

PHYSICAL REVIEW D VOLUME 5, NUMBER 7 1 APRIL 1972

Some Aspects of Single-Particle and Two-Particle Inclusive Reactions in 12.7-GeV/c K^+p and 7-GeV/c π^+p Collisions*

S. Stone, T. Ferbel,† P. Slattery, and B. Werner
Department of Physics and Astronomy, University of Rochester,‡ Rochester, New York 14627
(Received 23 June 1971; revised manuscript received 10 March 1972)

We present single-particle momentum spectra for π^-, K^0, $\bar{\Lambda}^0$, and Λ^0 particles produced in K^+p collisions at 12.7 GeV/c, and for π^- mesons produced in π^+p collisions at 7 GeV/c. We examine the correlations between the transverse and longitudinal momentum components of these particles and compare them to those expected as a result of momentum conservation alone. We also investigate the transverse-momentum correlations in two-particle inclusive reactions and discuss the underlying kinematic constraints on these correlations.

I. INTRODUCTION

Total cross sections for hadron-hadron collisions appear to remain relatively constant in the high-energy domain, and since the amount of quasi-two-body production decreases rapidly with increasing bombarding energy, the major part of high-energy total cross sections necessarily involves processes in which many final-state particles are produced. Consequently, the study of multiparticle reactions is an essential part of the investigation of high-energy processes. Although a detailed theoretical analysis of multiparticle reactions would be at present prohibitively complicated, Feynman, Yang, and others[1,2] have suggested that the characteristics of a single particle, summed over all final states, can yield important dynamical information concerning strong interactions. Such "inclusive" processes may be schematically represented by

$$a+b\to c+\text{anything}, \tag{1}$$

where c is the single particle being analyzed, and are the next level of sophistication above a total cross-section measurement which may be regarded as the analysis of the process

$$a+b\to\text{anything} \tag{2}$$

in which all final states are summed over. It has also been suggested[3] that more complicated processes in which two final-state particles are detected, and their momentum correlations analyzed, i.e., the processes

$$a+b\to c+d+\text{anything}, \tag{3}$$

may also be amenable to present theoretical analysis.

The theoretical application of Regge-pole ideas to inclusive reactions has implied that the momentum spectra of individual final-state particles approach limiting behavior differently in various kinematic regions. For example, in the region of target or beam fragmentation these limits are approached as $1/\sqrt{s}$, while in the central, or "pionization," region these limits are reached more slowly, approximately as $s^{-1/4}$. For two-particle inclusive reactions, the distribution in the correlation angle between the transverse momentum of the two particles is expected to approach limiting behavior as $1/\sqrt{s}$ in the appropriate single-Regge limit. Even at present accelerator energies, the $1/\sqrt{s}$ approach to asymptotic behavior may be rapid enough so that useful tests of the Regge ideas involved in these predictions may be carried out.

We present data from two[4,5] experiments utilizing the 80-in. BNL bubble chamber. The following reactions have been investigated:

$$K^+p\to\pi^-+\cdots, \quad 12.7\ \text{GeV}/c \tag{4}$$
$$K^+p\to K^0+\cdots, \quad 12.7\ \text{GeV}/c \tag{5}$$
$$K^+p\to\bar{\Lambda}^0+\cdots, \quad 12.7\ \text{GeV}/c \tag{6}$$
$$K^+p\to\Lambda^0+\cdots, \quad 12.7\ \text{GeV}/c \tag{7}$$
$$\pi^+p\to\pi^-+\cdots, \quad 7\ \text{GeV}/c \tag{8}$$
$$K^+p\to K^0+\pi^-+\cdots, \quad 12.7\ \text{GeV}/c \tag{9}$$
$$K^+p\to\bar{\Lambda}^0+\pi^-+\cdots, \quad 12.7\ \text{GeV}/c \tag{10}$$